Acta Pharmaceutica Sinica B 2019;9(1):128–134

Chinese Pharmaceutical Association
Institute of Materia Medica, Chinese Academy of Medical Sciences

Acta Pharmaceutica Sinica B

www.elsevier.com/locate/apsb
www.sciencedirect.com

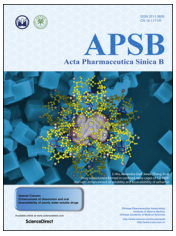

ORIGINAL ARTICLE

Preparation and characterization of multimodal hybrid organic and inorganic nanocrystals of camptothecin and gold ☆

Christin P. Hollis[a], Alan K. Dozier[b], Barbara L. Knutson[c], Tonglei Li[d,*]

[a]*Department of Pharmaceutical Sciences, University of Kentucky, Lexington, KY 40506, USA*
[b]*Electron Microscopy Center, University of Kentucky, Lexington, KY 40506, USA*
[c]*Department of Chemical Engineering and Material Sciences, University of Kentucky, Lexington, KY 40506, USA*
[d]*Department Industrial & Physical Pharmacy, College of Pharmacy, Purdue University, West Lafayette, IN 47907, USA*

Received 31 December 2017; received in revised form 15 February 2018; accepted 22 February 2018

KEY WORDS

Hybrid inorganic-organic;
Drug delivery;
Camptothecin;
Gold nanoparticles;
Computed tomography (CT) contrast agent;
Cancer therapy and diagnosis

Abstract We demonstrate a novel inorganic-organic crystalline nanoconstruct, where gold atoms were imbedded in the crystal lattices as defects of camptothecin nanocrystals, suggesting its potential use as simultaneous agents for cancer therapy and bioimaging. The incorporation of gold, a potential computed tomography (CT) contrast agent, in the nanocrystals of camptothecin was detected by transmission electron microscope (TEM) and further quantified by energy dispersive X-ray spectrometry (EDS) and inductively coupled plasma-optical emission spectrometers (ICP-OES). Due to gold's high attenuation coefficient, only a relatively small amount needs to be present in order to create a good noise-to-contrast ratio in CT imaging. The imbedded gold atoms and clusters are expected to share the same biological fate as the camptothecin nanocrystals, reaching and accumulating in tumor site due to the enhanced permeation and retention (EPR) effect.

*Corresponding author. Tel.: +1 765 4941451.
E-mail address: tonglei@purdue.edu (Tonglei Li).
☆Invited for Special Column.
Peer review under responsibility of Institute of Materia Medica, Chinese Academy of Medical Sciences and Chinese Pharmaceutical Association.

https://doi.org/10.1016/j.apsb.2018.03.005

1. Introduction

The development of multimodal nanomedicine, which combines the therapeutic and diagnostic capabilities, has tremendous potential to revolutionize the future of cancer therapy. By incorporating bio-imaging agent molecules, the delivery of therapeutic agent can be potentially monitored and traced *in vivo*. Over the past decade, the application of fluorescent markers, both organic- and inorganic-based material, has been vastly explored[1,2]. While organic dyes may suffer from limitations, such as photobleaching, biodegradation, and narrow excitation/broad emission spectra, the lack of biocompatibility and high toxicity hinders the utilization of the inorganic markers[3]. In addition, fluorescence imaging is still limited to *in vivo* studies due to low sensitivity and shallow optical path. Current imaging modalities, including positron emission tomography (PET), computed tomography (CT), magnetic resonance imaging (MRI), and ultrasound, can provide anatomical patterns and basic information regarding tumor location, size, and progression and are still the standard clinical tools[4,5].

Attributed to its availability, efficiency, and cost, X-ray based CT is among the most convenient imaging/diagnostic tools in hospitals today[6,13]. Iodinated aromatic molecules are the most commonly contrast agent used in clinics and dominate the X-ray contrast media markets[7,8]. Due to its rapid renal clearance, however, approximately 100–200 mL of highly concentrated iodinated contrast medium solution (*ca.* 600 mg/mL) are administered intravenously to achieve adequate contrast[8]. Adverse reactions caused by excessive amount of chemicals have also been reported[8–10]. In the past few years, the feasibility of using gold nanoparticles as a CT contrasting agent has been tested *in vivo*, both through passive[11,12] or active[12,13] targeting. Within a CT image, one can distinguish the difference between tissues based on the degrees of the X-ray attenuation; more X-rays are attenuated in denser tissues. The contrast of structure or fluid within the body can be enhanced by utilizing contrast agent, where its attenuation coefficient is determined by the atomic number and electron density. Because gold's atomic number and electron density (79 and 19.32 g/cm^3, respectively) are higher than iodine (53 and 4.9 g/cm^3, respectively), gold gives a higher mass attenuation coefficient. For instance, at 100 keV (a standard X-ray energy for diagnostic imaging), gold and iodine have attenuation coefficient of 5.16 and 1.94 cm^2/g, respectively[14]; thus, gold provides about 2.7 times stronger contrast per unit weight than iodine. In addition, the low toxicity and good biocompatibility[15] make gold (clusters and nanoparticles) an ideal contrast agent. More importantly, regardless the shape of gold nanoparticles, the only important parameter in CT imaging is the total amount of gold per unit volume[13]. The utilization of gold as contrast agent *in vivo* was first reported in 2006[12], and it is being continually explored.

In the past two decades, colloidal drug delivery systems (CDDS), including liposomes[16], solid lipid nanoparticles[17], polymeric nanoparticles[18], and micelles[19], have been used to formulate highly insoluble antic drugs. Despite the fact that these systems have been extensively studied, various inherent limitations remain. They generally have limited drug loading capacity[20,21]. Phospholipid-based structures, such as liposomes, may also suffer from drug leakage and instability during the preparation, storage, and administration process that can compromise the therapeutic outcomes[22,23]. As such, more physically stable and solvent-free nanocrystals-based formulation may be used for delivering antineoplastic drugs and reach the tumor site in the solid form. Nanocrystals formulated from poorly soluble drugs may not dissolve quickly[24], providing a potential vehicle or carrier for a contrast agent. This multimodal design may lead to cancer theranostic systems, which can be passively targeted to tumor site *via* enhanced permeation and retention (EPR) effect[25]. The fundamental concept of such an integrated crystalline system lies in physical inclusion of a bioimaging substance in the crystal lattices as defects of a host drug compound; no chemical conjugation is thereby needed. Herein, the purpose of this report is to demonstrate successful incorporation of gold ions or atoms and their clusters in the nanocrystals of a chemotherapeutic drug, camptothecin (CPT). The idea of this novel hybrid nanocrystal was inspired by the studies of "dyeing crystals"[26], where organic dyes are imbedded in organic crystals. To the best of our knowledge, purported incorporation of an inorganic material into organic nanocrystal lattices for biomedical applications has not been previously reported.

CPT was selected as the model drug because it has a broad spectrum of therapeutic activity against various cancer types[27,28]. Similar to other chemotherapeutic agents, CPT has a low solubility in water (*ca.* 1.2 μg/mL at 25 °C). It also has a well-established clinical and been the focus of numerous drug delivery studies since its discovery in 1966[29]. Specifically, the antitumor activity of CPT results from its ability to actively target and inhibit the DNA enzyme topoisomerase I (TOP1). Unfortunately, the clinical application of the drug remains greatly limited, largely due to its inherent instability in solution as well as protein binding in the plasma. The native, biologically active compound may undergo hydrolysis and produce an inactive form (Fig. 1). The ring-open reaction, which converts the lactone to carboxylate, occurs above pH 7. Despite the chemical instability of the molecule, pure CPT nanocrystals showed to accumulate in tumor and inflict the antitumor effect, as demonstrated in our recent study[30]. In our experiments reported here, preparation and storage of hybrid CPT nanocrystals were conducted in pH 4-water to maintain its active lactone form.

2. Materials and methods

2.1. Materials

Camptothecin (>99%) was purchased from 21CECPharm (UK); all other chemicals and solvents were obtained from Sigma (St.

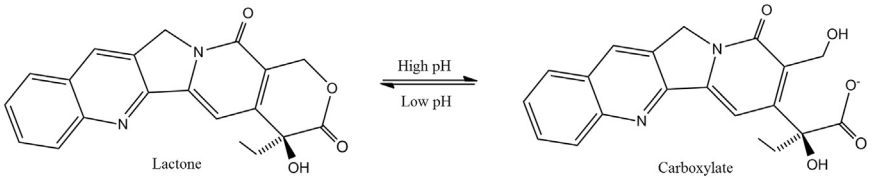

Figure 1 The two forms of camptothecin (CPT).

Louis, MO, USA) and Fisher Scientific (Pittsburgh, PA, USA). 200-mesh Lacey carbon grids were from Electron Microscopy Sciences (Hatfield, PA, USA).

2.2. *Preparation of hybrid nanocrystals*

To produce hybrid CPT/gold nanocrystals, 40 mL of boiled pH 4 water (adjusted with 0.25 mol/L HCl) and 3 mL of 1 mmol/L hydrogen tetrachloroaurate, $HAuCl_4$, were added together in a three-neck flask. The mixture was stirred at 500 rpm with a stirrer shaft and under intense sonication (F20D, Fisher Scientific, Pittsburgh, PA, USA). Next, 0.3 mL of 1% trisodium citrate dehydrate aqueous solution was added to the flask. While the gold salt solution was being reduced, 2 mL of 1 mg/mL CPT dimethyl sulfoxide (DMSO) solution was added. The system continued to be sonicated and stirred to promote crystal growth and gold reduction. The solution changed its color from clear to pinkish. To produce hybrid CPT/gold ions nanocrystals, the same procedure was performed except for the addition of 0.3 mL of 1% trisodium citrate dehydrate aqueous solution. As such, gold was entrapped in the CPT nanocrystals as ions (chloroaurate). Because of the absence of redox reaction, the solution and retentate remained colorless.

Once hybrid nanocrystals formed, the crystals were harvested by vacuum filtering with a 50-nm polycarbonate nuclepore filter. With the vacuum filtration system still intact, approximately 5 to 10 mL of pH 4 water was added to rinse off any gold atoms or ions that were not incorporated or attached to the nanocrystals. The product harvested on the filter was then re-suspended in pH 4 water by sonicating the filter paper. For further removal of free gold clusters or ions, the procedure of filtration, washing and re-suspension by sonication was repeated three more times. Following the final filtration process, the product collected on the filter paper was re-suspended in 1 mL of pH 4 water and diluted with aqua regia for gold analysis by inductively coupled plasma, or ICP (Vista-Pro ICP-OES, Varian, Palo Alto, CA, USA). Filtrate from each filtration process was also collected for mass balance calculation. Only trace amount of CPT and gold were present in the second and third filtrate; thus, only the first filtrate was analyzed by ICP. Before mixing with the digestion solution, filtrate was concentrated by boiling the water, leaving a total volume of 5 mL.

2.3. *Analysis of hybrid nanocrystals*

The Varian Vista-Pro ICP-OES was utilized to quantify the amount of the gold incorporated. 1 mL of either the concentrated product or filtrate was dissolved with 1 mL of freshly mixed aqua regia (1:3 mixture of concentrated nitric acid and hydrochloric acid) and diluted with 3 mL of deionized water. Standard solutions were prepared by using ICP standard for gold (Fisher Scientific, Pittsburgh, PA, USA) diluted with aqua regia at concentrations of 0.010, 0.050, 0.1, 0.5, 1, 5, 10, and 50 ppm. Analysis was performed at wavelength of 267 nm. Quantification of CPT was conducted by high-pressure liquid chromatography (HPLC, Waters Breeze, Milford, MA, USA) with UV detection (Waters 2487 dual λ absorbance detector) at 256 nm. A Waters' Symmetry C18 5 μm column (150 mm × 4.6 mm) was used at 33 °C with a mixture (36:64) of acetonitrile and 2% triethylamine aqueous solution, adjusted to pH 5.5 by acetic acid, as the mobile phase pumped at a rate of 0.5 mL/min (Waters 1525 binary pump).

2.4. *Electron microscopy imaging and energy dispersive X-ray spectroscopy (EDS)*

SEM images were obtained using Hitachi SEM 4300 (Tokyo, Japan) at an accelerating voltage of 3 kV. Prior to visualization, samples were coated with conductive layers of gold palladium (Au/Pd) for 1 min with current of 20 mA in a sputter coater, resulting in approximately 15 nm thick coating. The coating helped

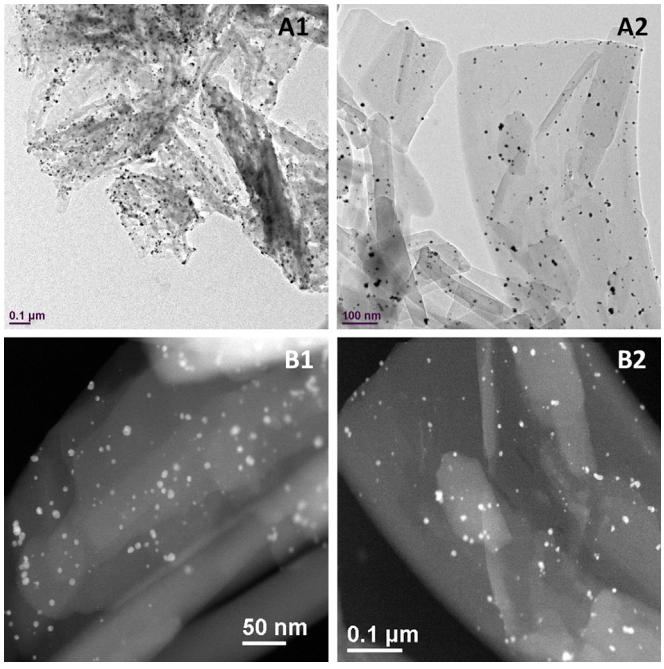

Figure 2 TEM (A) and STEM (B) images of CPT/gold hybrid nanocrystals without vigorous washing and filtering.

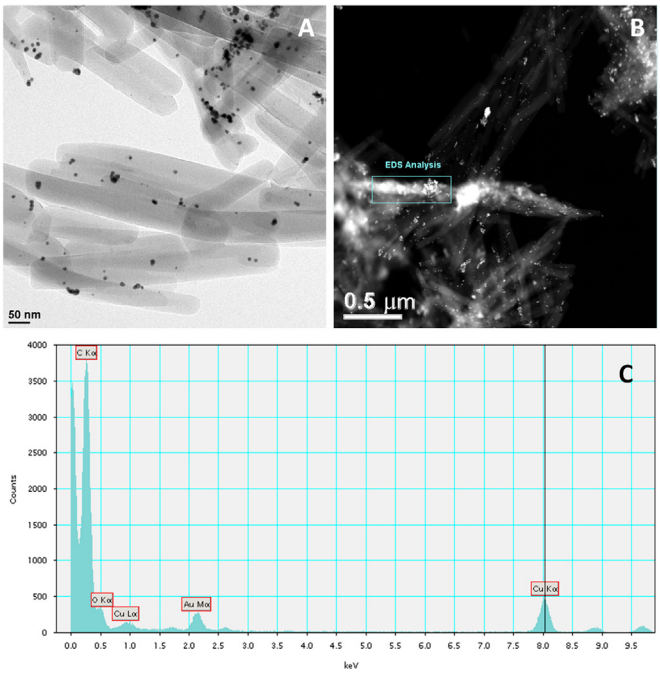

Figure 3 TEM (A) and STEM (B) images of CPT/gold hybrid nanocrystals after vigorous washing and filtering. An EDS spectrum of the area highlighted in (B) is shown in (C).

to reduce sample charging. The freeze-dried hybrid nanocrystals were imaged by using JEOL 2010F TEM (JEOL USA, Peabody, MA, USA) equipped with an Oxford EDS detector. TEM was operated at 200 keV. Scanning Transmission Electron Microscopy (STEM) was performed at high angle conditions of approximately 50 mrad, using a 1.7 Å high resolution probe. EDS was performed under STEM conditions using a 1 nm analytic probe. A small amount of the freeze dried hybrid nanocrystals were rubbed on the Lacey carbon grid and placed in the sample holder for imaging. Samples obtained after one cycle of washing and re-suspension was compared to that washed and re-suspended three times.

3. Results and discussion

Incorporation of gold in CPT nanocrystals was attempted in two ways to retain gold atoms or gold ions. Both preparations were conducted in a single step, eliminating typical multi-step chemical treatment of conjugating bio-imaging agents[31,32]. To make hybrid nanocrystals of CPT and gold atoms, chloroauric acid was reduced concurrently when the nucleation of camptothecin nanocrystals was triggered *via* the anti-solvent method. The redox reaction was based on a simple route developed by McFarland et al.[33], where citrate aqueous solution was added to reduce the chloroauric acid. It is believed that the reduced gold was integrated into CPT nanocrystals as individual atoms and clusters. As the reduction progressed, the solution changed from clear to pinkish. While the reducing agent was introduced, a high concentration of dissolved CPT in dimethyl sulfoxide (DMSO) was added to the aqueous media of pH 4, resulting in nucleation and growth of CPT nanocrystals. In the case of incorporating gold ions, citrate solution was not added. Thus, without the reduction step, individual or clusters of chloroauric acid are believed to be entrapped in the crystal lattices of the CPT nanocrystals. At the end of each batch process, product was filtered with 50-nm polycarbonate filter paper and freeze-dried either with (Fig. 2) or without (Fig. 3) extra washing and re-suspension step.

The hybrid camptothecin nanocrystals had morphology of rectangular thin sheet, with the length ranged from approximately 300 nm to 1.5 µm (Fig. 2). The exact average size could not be precisely determined by dynamic light scattering (DLS) because of the nanocrystals' high aspect ratio. The TEM and STEM images (Fig. 2) clearly showed that gold clusters were attached and incorporated to the organic nanocrystals with high affinity, even after vigorous washing and sonicating (Fig. 3). Visually, the hybrid nanocrystals seem to be aggregated, possibly due to the freeze drying process. The size of the imbedded gold atom clusters was approximately 10 nm (Figs. 2 and 3), consistent with the size reported by McFarland et al.[33] EDS analysis of the gold clusters in the CPT nanocrystals revealed that the expected characteristic peaks of oxygen (O), carbon (C), gold (Au), and copper (Cu) were present. The oxygen and carbon peaks were due to the drug, CPT, and the copper peak was due to the TEM sample holder.

In the absence of reduction of chloroauric acid during the nanocrystal preparation, individual or clusters of gold ions (chloroaurate) were incorporated in the camptothecin nanocrystals (Fig. 4A). The clusters of these ions were approximately 1.4 nm in size (Fig. 4B and B*), and the individual gold ions seen as white spots were approximately 2 Å in diameter (Fig. 4C and C*). The white spots are believed to be individual gold ions incorporated as crystal defects of the camptothecin nanocrystals. If these ions were not imbedded in the crystals, they would have been washed off by the sonication step. The gold ions were also shown to be more homogenously distributed relative to that of the reduced gold atoms/clusters (Figs. 2 and 3). EDS analyses showed peaks of both gold and chlorine. Fast Fourier Transform (FFT) image processing was utilized to get more a detailed and optimized structure image of the hybrid camptothecin nanocrystal (Fig. 5). In this analysis, a Fourier transform was applied to Fig. 5A producing the diffractogram Fig. 5C. The diffraction spots were then filtered as in

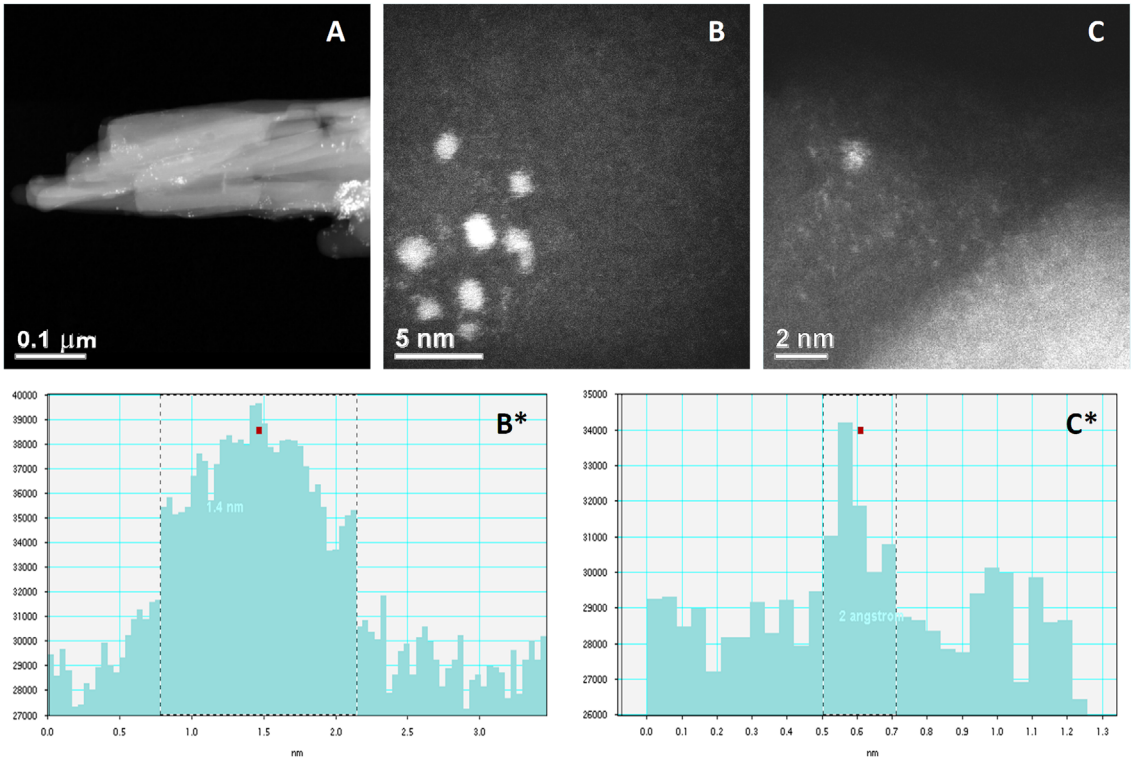

Figure 4 STEM images of CPT/chloroaurate hybrid nanocrystals after vigorous washing and filtering. (A) Individual or clusters of gold ions (chloroaurate) were incorporated in the camptothecin nanocrystals. (B) shows clusters of gold ions, and (C) shows individual gold ions. Particle analysis results of the white dots in (B) and (C) are shown in (B*) and (C*), respectively.

Fig. 5D, and an inverse Fourier transform applied producing image Fig. 5B. This brings out the CPT lattice planes giving a lattice spacing of approximately 4 Å.

The percent entrapment of gold in the camptothecin nanocrystals was quantified by inductively coupled plasma-optically emission spectrometry (ICP-OES)[34]. Relative to the amount of the starting material, 8.11% and 1.31% of gold atoms and chloroauric acid (Table 1), respectively, were present in the hybrid nanocrystals. The reduction process allows neutral gold clusters to form quickly and to be entrapped to the camptothecin nanocrystals. On the other hand, chloroaurate incorporation may be relatively limited due to its ionized state in the solution and the need to bind a counter ion (most likely, proton) prior to the entrapment. As such, more gold atoms were integrated in the CPT nanocrystals (Table 1). Note that these nanocrystals were vigorously washed under sonication and re-filtered for multiple times, so the majority of quantified gold atoms or ions were imbedded as chemical impurity as defects in the crystal structure. The same phenomenon is observed routinely in the nature. Colored diamonds and gemstones originated when impurities are trapped in the lattice defects. Interestingly enough, in the case of colored diamond, impurities (*e.g.*, N) can still be introduced in the exceptionally strong diamond's lattice. Because of the rapid nucleation and growth, the CPT nanocrystals may have more crystal defects and thus incorporate more gold atoms/ions and their clusters.

The percentage of gold integration in the CPT nanocrystals may permit bioimaging. Because of the sensitivity of CT imaging and the high attenuation coefficient of gold, a good contrast-to-noise image can be obtained at gold concentration of 100 μg/mL[12,35], which is approximately a hundred times lower than the cytotoxicity of gold nanoparticles. It is important to note that even at its low dosing, gold can exhibit longer blood retention (*i.e.*, allowing prolonged imaging time) due to its inherent physical property of high molecular weight[12]. Nonetheless, it seems that our hybrid nanocrystals provide a much less amount of gold *in vivo*. Given the largest loading percentage of gold in the CPT nanocrystals, 3.47% (Table 1), there would be 10.4 μg of gold delivered to a mouse (at a typical intravenous dosing level of 100 μL × 3 mg/mL of CPT), which is an order of magnitude less than the reported value for obtaining good CT imaging (assuming that the blood volume of a mouse is 1.2 mL)[12,35]. Still, considering the additional advantages of maximizing integrity and minimizing clearance of gold established by its entrapment in nanocrystals, which have been shown to accumulate in the tumor because of the leaky vasculatures present inside tumorous tissues and underdeveloped lymphatic drainage (*i.e.*, the EPR effect), the local gold concentration may be higher enough for CT imaging of cancer. In fact, it is reported that the vascular pore cutoff size (*i.e.*, transvascular gaps) in the majority of tumors are between 380 and 780 nm, and it can go as high as between 1.2 and 2 μm in MCa IV, murine mammary carcinoma[36,37]. Our recent study of pure CPT nanocrystals in a mouse tumor model has supported the tumor targeting and antitumor capability of the nanocrystals[30]. In addition, the hybrid nanocrystals can be delivered without the need of using toxic solubilizing agents, likely resulting in the maximum tolerated dose (MTD) by five to ten folds relative to conventional delivery

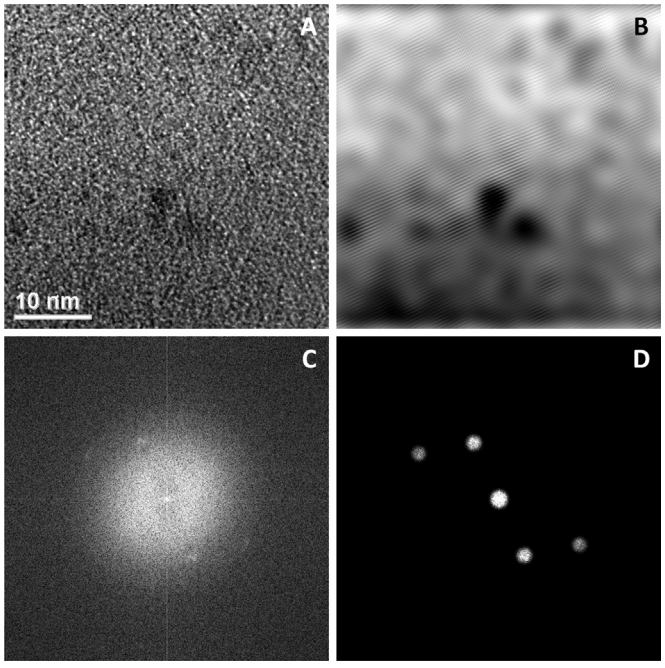

Figure 5 High-resolution TEM image of hybrid CPT nanocrystals (A) and its diffractogram (C). The diffractogram is further noise-filtered (D), which is then inversely Fourier transformed (B).

systems that are prepared with organic solvents, surfactants, or complexing compounds (*e.g.*, cyclodextrin)[24]. The feasibility of hybrid camptothecin/gold nanocrystals as a cancer theranostic system will of course need to be further tested *in vivo*. With this proof-of-concept at hand, alternate route including irradiating the imbedded gold (or other inorganic elements such as samarium) and converting to its radioisotope[198], Au, may be pursued for radio-imaging modalities.

4. Conclusions

Herein, we have demonstrated that gold, an inorganic material, can be incorporated in the nanocrystals of an organic compound, camptothecin in two different forms, atom and ion. Specifically, gold was imbedded as the defects in crystal lattices and the hybrid constructs could withstand multiple cycles of vigorous washing, filtering, and re-suspension (under sonication) to retain the guest substance. Incorporation of individual gold ion, as small as 2 Å was able to be imaged by TEM. The concept of integrating inorganic materials into organic nanocrystals likely leads to creation of novel theranostic systems for combating cancers. While high attenuation inorganic materials, such as gold, can be utilized as contrast imaging agents, inorganic radioisotopes can also be integrated in a similar fashion in drug nanocrystals for other types of bioimaging applications.

Table 1 ICP analysis of gold entrapment in hybrid CPT/gold nanocrystals.

	% *w/w* incorporation relative to the starting material (% Efficiency)	% *w/w* incorporation relative to the amount of camptothecin (% Loading)
With redox	8.11	3.47
Without redox	1.31	1.06

Acknowledgments

This work was supported by Department of Defense Breast Cancer Research Program (DOD BCRP #BC050287). NSF IGERT) Bioactive Interface and Devices.

References

1. Sukhanova A, Nabiev I. Fluorescent nanocrystal-encoded microbeads for multiplexed cancer imaging and diagnosis. *Crit Rev Oncol-Hemtol* 2008;**68**:39–59.
2. Sharrna P, Brown S, Walter G, Santra S, Moudgil B. Nanoparticles for bioimaging. *Adv Colloid Interface Sci* 2006;**123**:471–85.
3. Weng KC, Noble CO, Papahadjopoulos-Sternberg B, Chen FF, Drummond DC, Kirpotin DB, et al. Targeted tumor cell internalization and imaging of multifunctional quantum dot-conjugated immunolipo-somes *in vitro* and *in vivo*. *Nano Lett* 2008;**8**:2851–7.
4. Choi HJ, Ju W, Myung SK, Kim Y. Diagnostic performance of computer tomography, magnetic resonance imaging, and positron emission tomography or positron emission tomography/computer tomography for detection of metastatic lymph nodes in patients with cervical cancer. Meta-analysis. *Cancer Sci* 2010;**101**:1471–9.
5. Basu S, Li GM, Alavi A. PET and PET-CT imaging of gynecological malignancies: present role and future promise. *Expert Rev Anticancer* 2009;**9**:75–96.
6. Weber WA, Grosu AL, Czernin J. Technology insight: advanaces in molecular imaging and an appraisal of PET/CT scanning. *Nat Clin Pract Oncol* 2008;**5**:160–70.
7. Eck W, Nicholson AI, Zentgraf H, Semmler W, Bartling S. Anti-CD4-targeted gold nanoparticles induce specific contrast enhancement of peripheral lymph nodes in X-ray computed tomography of live mice. *Nano Lett* 2010;**10**:2318–22.

8. Christiansen C. X-ray contrast media-an overview. *Toxicology* 2005;**209**:185–7.
9. Hosoya T, Yamaguchi K, Akutsu T, Mitsuhashi Y, Kondo S, Sugai Y, et al. Delayed adverse reactions to iodinated contrast media and their risk factors. *Radiat Med* 2000;**18**:39–45.
10. Katayama H, Yamaguchi K, Kozuka T, Takashima T, Seez P, Matsuura K. Adverse reactions to ionic and nonionic contrast media. A report from the Japanese committee on the safety of contrast media. *Radiology* 1990;**175**:621–8.
11. Hainfeld JF, Slatkin DN, Smilowitz HM. The use of gold nanoparticles to enhance radiotherapy in mice. *Phys Med Biol* 2004;**49**:N309–15.
12. Hainfeld JF, Slatkin DN, Focella TM, Smilowitz HM. Gold nanoparticles: a new X-ray contrast agent. *Br J Rad* 2006;**79**:248–53.
13. Popovtzer R, Agrawal A, Kotov NA, Popovtzer A, Balter J, Carey TE, et al. Targeted gold nanoparticles enable molecular CT imaging of cancer. *Nano Lett* 2008;**8**:4593–6.
14. physics.nist.gov [Internet]. Gaithersburg: National Institute of Standards and Technology (NIST) [Accessed 10 December 2017]. Available from: ⟨http://physics.nist.gov/PhysRefData/XrayMassCoef⟩.
15. Connor EE, Mwamuka J, Gole A, Murphy CJ, Wyatt MD. Gold nanoparticles are taken up by human cells but do not cause acute cytotoxicity. *Small* 2005;**1**:325–7.
16. Harrington KJ. Liposomal cancer chemotherapy: current clinical applications and future prospects. *Expert Opin Investig Drugs* 2001;**10**:1045–61.
17. Puri A, Loomis K, Smith B, Lee JH, Yavlovich A, Heldman E, et al. Lipid-based nanoparticles as pharmaceutical drug carriers: from concepts to clinic. *Crit Rev Ther Drug Carr Syst* 2009;**26**:523–80.
18. Tong R, Cheng JJ. Anticancer polymeric nanomedicines. *Polym Rev* 2007;**47**:345–81.
19. Sutton D, Nasongkia N, Blanco E, Gao JM. Functionalized micellar systems for cancer targeted drug delivery. *Pharm Res* 2007;**24**:1029–46.
20. Torchilin VP. Micellar nanocarriers: pharmaceutical perspectives. *Pharm Res* 2007;**24**:1–16.
21. Garcia-Fuentes M, Alonso MJ, Torres D. Design and characterization of a new drug nanocarrier made from solid-liquid lipid mixtures. *J Colloid Interface Sci* 2005;**285**:590–8.
22. Mayer LD, Krishna R, Webb M, Bally M. Designing liposomal anticancer drug formulations for specific therapeutic applications. *J Liposome Res* 2000;**10**:99–115.
23. Gulati M, Grover M, Singh S, Singh M. Lipophilic drug derivatives in liposomes. *Int J Pharm* 1998;**165**:129–68.
24. Merisko-Liversidge E, Liversidge GG, Cooper ER. Nanosizing: a formulation approach for poorly-water-soluble compounds. *Eur J Pharm Sci* 2003;**18**:113–20.
25. Maeda H. The enhanced permeability and retention (EPR) effect in tumor vasculature: the key role of tumor-selective macromolecular drug targeting. *Adv Enzym Regul* 2001;**41**:189–207.
26. Kahr B, Gurney RW. Dyeing crystals. *Chem Rev* 2001;**101**:893–951.
27. Garcia-Carbonero R, Supko JG. Current perspectives on the clinical experience, pharmacology, and continued development of the camptothecins. *Clin Cancer Res* 2002;**8**:641–61.
28. Sriram D, Yogeeswari P, Thirumurugan R, Bal TR. Camptothecin and its analogues: a review on their chemotherapeutic potential. *Nat Prod Res* 2005;**19**:393–412.
29. Adams VR, Burke TG. *Camptothecins in Cancer Therapy*. Danvers, MA: Humana Press Inc.; 2005.
30. Zhang H, Hollis CP, Zhang Q, Li T. Preparation and antitumor study of camptothecin nanocrystals. *Int J Pharm* 2011;**415**:293–300.
31. Chen WX, Bardhan R, Bartels M, Perez-Torres C, Pautier RG, Halas NJ, et al. A molecularly targeted theranostic probe for ovarian cancer. *Mol Cancer Ther* 2010;**9**:1028–38.
32. Guo R, Li R, Zhang L, Jiang X, Liu B. Dual-functional alginic acid hybrid nanospheres for cell imaging and drug delivery. *Small* 2009;**5**:709–17.
33. McFarland AD, Haynes CL, Mirkin CA, van Duyne RP, Godwin HA. Color my nanoworld. *J Chem Ed* 2004;**81**:544A.
34. Liu YL, Shipton MK, Ryan J, Kaufman ED, Franzen S, Feldheim DL. Synthesis, stability, and cellular internalization of gold nanoparticles containing mixed peptide-poly(ethylene glycol) monolayers. *Anal Chem* 2007;**79**:2221–9.
35. Dilmanian FA, Wu XY, Parsons EC, Ren B, Kress J, Button TM, et al. Single- and dual-energy CT with monochromatic synchrotron X-rays. *Phys Med Biol* 1997;**42**:371–87.
36. Hobbs SK, Monsky WL, Yuan F, Roberts WG, Griffith L, Torchilin VP, et al. Regulation of transport pathways in tumor vessels: role of tumor type and microenvironment. *Proc Natl Acad Sci U S A* 1998;**95**:4607–12.
37. Hashizume H, Baluk P, Morikawa S, McLean JW, Thurston G, Roberge S, et al. Opening between defective endothelial cells explain tumor vessel leakiness. *Am J Pathol* 2000;**156**:1363–80.